DESY 25-127, ZU-TH 59/25, MPP-2025-182, RISC Report Series 25–08, arXiv:2509.16124 [hep-ph]

The three-loop single-mass heavy-flavor corrections to the structure functions $F_2(x,Q^2)$ and $g_1(x,Q^2)$

J. Ablinger,[1] A. Behring,[2] J. Blümlein,[3,4] A. De Freitas,[1] A. von Manteuffel,[5] C. Schneider,[1] and K. Schönwald[6]

[1] *Johannes Kepler University Linz, Research Institute for Symbolic Computation (RISC), Altenberger Straße 69, A-4040, Linz, Austria*

[2] *Max-Planck-Institut für Physik (Werner-Heisenberg-Institut), Boltzmannstraße 8, 85748 Garching, Germany*

[3] *Deutsches Elektronen-Synchrotron DESY, Platanenallee 6, 15738 Zeuthen, Germany*

[4] *Institut für Theoretische Physik III, IV, TU Dortmund, Otto-Hahn Straße 4, 44227 Dortmund, Germany*

[5] *Institut für Theoretische Physik, Universität Regensburg, 93040 Regensburg, Germany*

[6] *Physik-Institut, Universität Zürich, Winterthurerstraße 190, CH-8057 Zürich, Switzerland*

We report quantitative results on the single-mass heavy-flavor contributions up to three-loop order to the unpolarized structure function $F_2(x,Q^2)$ and the polarized structure function $g_1(x,Q^2)$ for the first time. These results are relevant for precision QCD analyses of the World deep-inelastic data and the data taken at future colliders, such as the Electron–Ion Collider, in order to measure the strong coupling constant $\alpha_s(M_Z^2)$, and the twist-2 parton distribution functions consistently at next-to-next-to-leading order.

INTRODUCTION

The heavy-flavor corrections to deep-inelastic structure functions form an essential contribution in the region of smaller values of Bjorken x. Their scaling violations are quite different from those of the massless contributions, which requires their detailed knowledge in QCD precision analyses of these structure functions, such as the precision measurement of the strong coupling constant $a_s = \alpha_s/(4\pi) = g_s^2/(16\pi^2)$ [1–4], the charm quark mass m_c [5], and the parton distribution functions, cf., e.g., Refs. [6–8].

With the final results on the next-to-next-to-leading order (NNLO) single-mass corrections to the heavy-flavor Wilson coefficients in the region $Q^2 \gg m_Q^2$, with m_Q the heavy quark mass, first predictions on the structure functions F_2 and g_1 can be made at this order. The massive Wilson coefficients can be represented by Mellin convolutions of the massive operator matrix elements (OMEs)

$$(\Delta)A_{ij} = \delta_{ij} + \sum_{k=1}^{\infty} a_s^k (\Delta) A_{ij}^{(k)} \tag{1}$$

and pieces of the massless Wilson coefficients, cf. [9, 10]. The massive OMEs have been calculated to three-loop order in the upolarized [11–16] and polarized cases, [12, 15–18][1]

Beyond the massive OMEs contributing to the massive Wilson coefficients, there are also others, $(\Delta)A_{gq,Q}$ and $(\Delta)A_{gg,Q}$, playing a role in the variable flavor number scheme [14, 32–36],

[1] The one– and two–loop corrections were calculated in Refs. [19–24] and [9, 25–31].

It has been shown in Ref. [9] that for the structure function $F_2(x,Q^2)$ the heavy-flavor corrections in the asymptotic region $Q^2 \gg m_Q^2$ agree with the complete result at the level of $O(1\%)$ if $Q^2/m_Q^2 > 10$ at two-loop order. This cut also safely removes the higher-twist effects, cf. Refs. [37–39].

The structure function $F_2(x,Q^2)$ consists of the massless part, $F_2^{\rm light}(x,Q^2)$ for the light flavors, and the massive part, $F_2^{\rm heavy}(x,Q^2)$, where the Wilson coefficients have either a charm or a bottom quark contribution.

$$F_2(x,Q^2) = F_2^{\rm light}(x,Q^2) + F_2^{c}(x,Q^2) + F_2^{b}(x,Q^2). \tag{2}$$

In our illustrations, we work in the fixed flavor number scheme for $N_F = 3$ light flavors with charges e_k. The formal structures are the same for the structure functions $F_2(x,Q^2)$ and $g_1(x,Q^2)$, and are obtained by substituting the unpolarized building blocks with the polarized ones. For $g_1(x,Q^2)$ the prefactor x in Eqs. (3,7) has to be replaced by 1/2.

The light flavor part of F_2 is given by [40, 41]

$$\begin{aligned} F_2^{\rm light}(x,Q^2) = x \sum_{k=0}^{N_F} e_k^2 \Bigg\{ \frac{1}{N_F} \Bigg[& C_{2,q}^{\rm S}\left(x,\frac{Q^2}{\mu^2}\right) \otimes \Sigma(x,\mu^2) \\ & + C_{2,g}^{\rm S}\left(x,\frac{Q^2}{\mu^2}\right) \otimes G(x,\mu^2) \Bigg] \\ & + C_{2,q}^{\rm NS}\left(x,\frac{Q^2}{\mu^2}\right) \otimes \Delta_k(x,\mu^2) \Bigg\}, \end{aligned} \tag{3}$$

where $\Delta_k(x,\mu^2), \Sigma(x,\mu^2)$ and $G(x,\mu^2)$ denote the non-singlet, singlet and gluon distribution with

$$\Delta_k(x,\mu^2) = f_k(x,\mu^2) + \bar{f}_k(x,\mu^2) - \frac{1}{N_F}\Sigma(x,\mu^2), \tag{4}$$

$$\Sigma(x,\mu^2) = \sum_{k=1}^{N_F} [f_k(x,\mu^2) + \bar{f}_k(x,\mu^2)], \tag{5}$$

with $f_{k,(\bar{k})}$ the quark and antiquark densities, and μ denotes the factorization scale. The unpolarized massless Wilson coefficients $C_{2,i}^j$ were calculated to three-loop order in Refs. [40, 41] and the polarized ones $\Delta C_{1,i}^j$ in Ref. [41]. The heavy-flavor part is given by, cf. Ref. [10],

$$\begin{aligned} &F_2^Q(x,Q^2) = \\ &x\Bigg\{\sum_{k=0}^{N_F} e_k^2 \Bigg[L_{2,q}^{\rm NS}(x) \otimes (f_k(x,\mu^2) + f_{\bar{k}}(x,\mu^2)) \\ &+\frac{1}{N_F}\left(L_{2,q}^{\rm PS}(x) \otimes \Sigma(x,\mu^2) + L_{2,g}^{\rm S}(x) \otimes G(x,\mu^2)\right)\Bigg] \\ &+e_Q^2\Bigg[H_{2,q}^{\rm PS}(x) \otimes \Sigma(x,\mu^2) + H_{2,g}^{\rm S}(x) \otimes G(x,\mu^2)\Bigg]\Bigg\}. \end{aligned} \tag{6}$$

It contains both flavor non-singlet and singlet contributions[2] Here we have suppressed the dependence on Q^2, m_Q^2 and μ^2 in the heavy-flavor Wilson coefficients H_i and L_i, and $\otimes$ denotes the Mellin convolution[3]

$$A(x) \otimes B(x) = \int_0^1 dx_1 \int_0^1 dx_2 \delta(x - x_1 x_2) A(x_1) B(x_2). \tag{7}$$

In Mellin space, the massive Wilson coefficients are polynomials of the expansion coefficients of the massive OMEs $(\Delta)A_{ij}$ and expansion coefficients of the massless Wilson coefficients, see Refs. [10, 14]. The massless Wilson coefficients to three-loop order can all be expressed in terms of either harmonic sums [44, 45] in Mellin space or harmonic polylogarithms [46] in x-space. For the massive Wilson coefficients, this only applies to the N_F-contributions [11] and to $(\Delta)L_q^{\rm NS}, (\Delta)L_q^{\rm PS}$ and $(\Delta)L_g^{\rm S}$. The pure singlet Wilson coefficient $(\Delta)H_q^{\rm PS}$ depends on generalized harmonic sums [47, 48] in Mellin space and can be cast into harmonic polylogarithms with changed argument in x-space. The gluonic Wilson coefficients $(\Delta)H_g^{\rm S}$ receive also finite binomial sum [49] and higher transcendental function contributions in Mellin space. They contain square-root valued iterated integrals [49] and ${}_2F_1$-solutions [50] in x-space.[4] Since we calculate the heavy-flavor corrections to inclusive structure functions, there are also contributions with massless final states, but virtual heavy-flavor corrections.

[2] For the study of pure non-singlet structure functions, see Ref. [42]. There the heavy flavor corrections are small.
[3] For the evaluation of the convolution integrals we use the integrator of Ref. [43].
[4] For surveys on the different mathematical structures and the used computer algebraic methods see Refs. [51, 52].

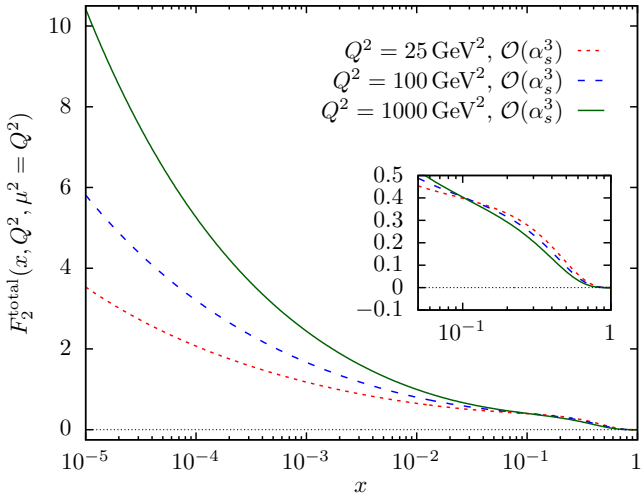

FIG. 1. The structure function $F_2(x,Q^2)$ at NNLO.

THE STRUCTURE FUNCTION $F_2(x,Q^2)$

In the unpolarized case, we use the parton distribution functions (PDFs) of Ref. [7] for $N_F = 3$. For the values of α_s in the Wilson coefficients, we use flavor matching with the values $\alpha_s(25\ \mathrm{GeV}^2) = 0.2020, \alpha_s(10^2\ \mathrm{GeV}^2) = 0.1706$, and $\alpha_s(10^3\ \mathrm{GeV}^2) = 0.1359$, corresponding to $\alpha_s(M_Z^2) = 0.1147$, consistent with the PDF fits. The massive Wilson coefficients were calculated referring to on-shell heavy quark masses. We use the following values

$$m_c = 1.59\ \mathrm{GeV}, \qquad m_b = 4.78\ \mathrm{GeV}, \tag{8}$$

cf. Refs. [5, 53].

In Figure 1, we illustrate the prediction for the total structure function $F_2^{\rm total}(x,Q^2)$, including the single-mass charm and bottom quark contributions. In the region $x \sim 10^{-5}$, it rises from $Q^2 = 25\ \mathrm{GeV}^2$ to $Q^2 = 1000\ \mathrm{GeV}^2$ from values of ~ 3.5 to 10.5. Around $x = 0.1$ there is a turning point above which the structure function takes lower values for larger values of Q^2.

Figure 2 shows the contributions of the different heavy-flavor Wilson coefficients to F_2^c at $Q^2 = 100\ \mathrm{GeV}^2$. The different lines illustrate also the contributions from $O(a_s)$ to $O(a_s^3)$ to the structure function. The largest contribution is due to the gluonic Wilson coefficient $H_g^{\rm S}$ which was scaled down by a factor of 20 for better readability. The corrections are positive and grow with the order in a_s. It is followed in size by a negative contribution from the pure-singlet Wilson coefficient $H_q^{\rm PS}$, which starts at $O(a_s^2)$. In the large-x region, the non-singlet Wilson coefficient $L_q^{\rm NS}$ yields the dominant part. However, the corrections compared to $F_2^{c,b}$ stay rather small. The corrections can become negative since virtual effects of heavy quarks with massless final states are contained in F_2^c and F_2^b. Also the contributions of $L_g^{\rm S}$ and $L_g^{\rm PS}$ are of importance at the level of accuracies of $O(1\%)$. $L_g^{\rm S}$ is tiny at

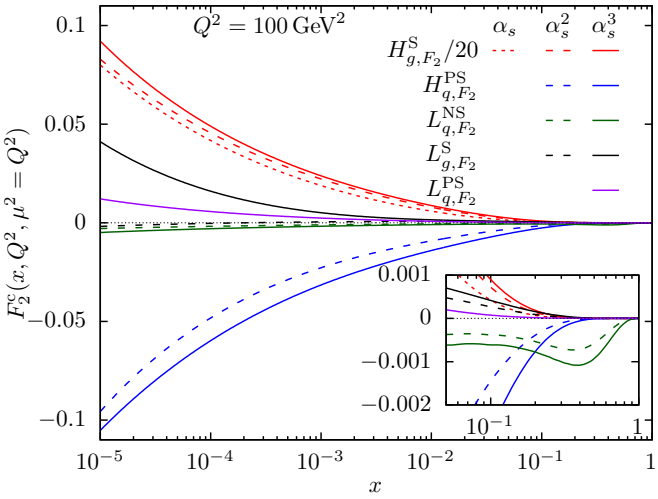

FIG. 2. The different heavy-flavor contributions due to charm quarks to the structure function $F_2(x,Q^2)$ by the Wilson coefficients $H_g^{\mathrm{S}}, H_q^{\mathrm{PS}}, L_q^{\mathrm{NS}}, L_g^{\mathrm{S}}$ and L_g^{PS} at $Q^2 = 100$ GeV^2 at different cumulative orders in a_s.

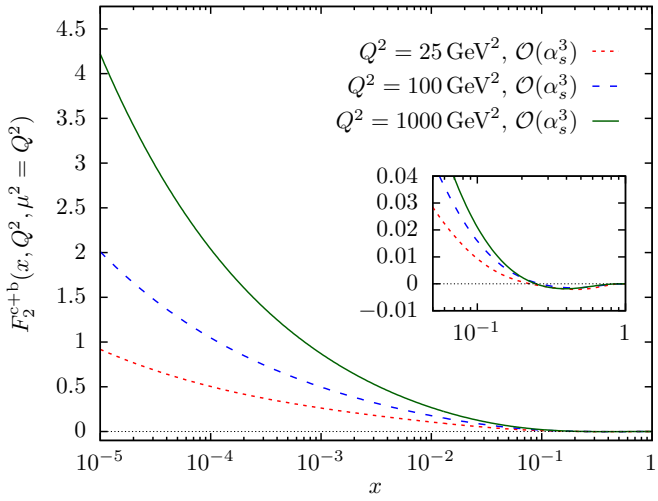

FIG. 3. The heavy-flavor contributions due to charm and bottom quarks to the structure function $F_2(x,Q^2)$ at NNLO.

$O(a_s^2)$, but receives a relative large correction at $O(a_s^3)$. A part of Wilson coefficients emerging at higher order in the coupling constant a_s can be negative as long as the unpolarized structure function remains positive.

In Figure 3 the heavy-flavor corrections to $F_2(x,Q^2)$ are shown at NNLO. At $x = 10^{-5}$, they grow from 1 to ~ 4 for $Q^2 = 25$ GeV^2 to $Q^2 = 1000$ GeV^2. In the large-x region the corrections are negative.

The relative single-mass charm and bottom contributions to $F_2(x,Q^2)$ are shown in Figure 4, as the ratio

$$R = \frac{F_2^c + F_2^b}{F_2^{\mathrm{light}} + F_2^c + F_2^b}, \tag{9}$$

at NNLO. In the small-x region of $x \sim 10^{-5}$, the fractions

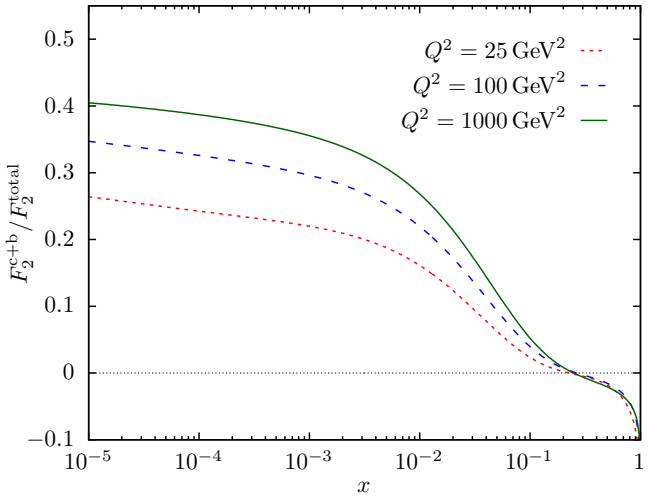

FIG. 4. The ratio of the heavy-flavor contributions due to charm and bottom quarks to the structure function $F_2(x,Q^2)$ at NNLO.

of the heavy-flavor corrections evolve from $Q^2 = 25$ GeV^2 to $Q^2 = 1000$ GeV^2 from 26 % to 41 %. At $x \sim 0.2$, the heavy-flavor corrections become zero, which is due to a combination of real and virtual corrections at NLO and NNLO. In the very-large-x region, the heavy-flavor contributions at NNLO become negative and as large as -10%, but the structure function F_2 itself remains non-negative. It is clearly seen that the scaling violations of the massive contributions are rather different compared to those in the massless case up to high values of Q^2.

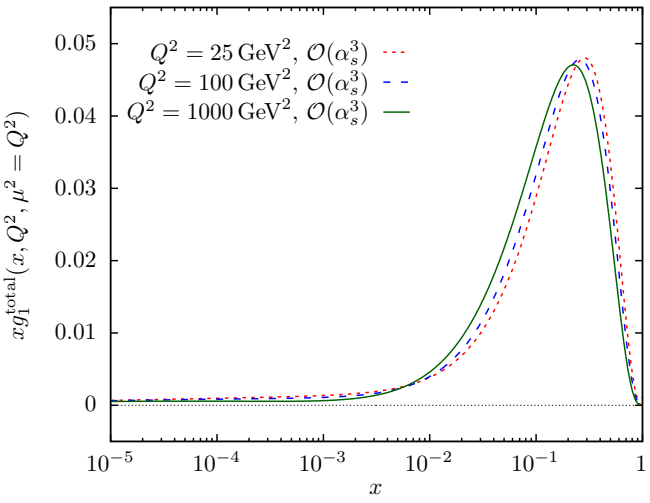

FIG. 5. The structure function $g_1(x,Q^2)$ at NNLO.

THE STRUCTURE FUNCTION $g_1(x,Q^2)$

In the polarized case the calculation is performed in the Larin scheme [54]. Both for the massive three-loop

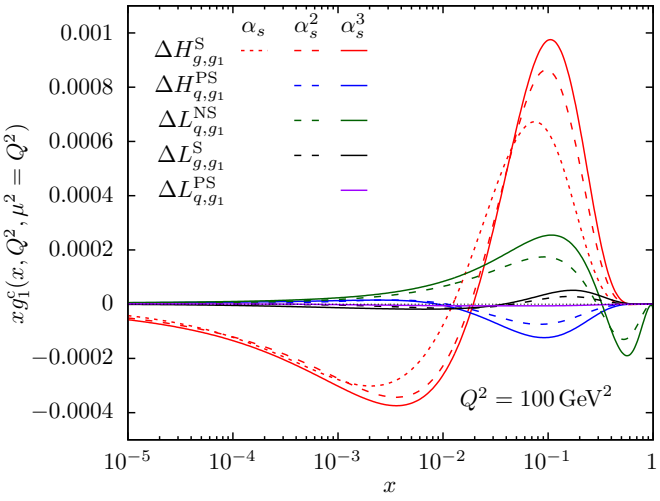

FIG. 6. The different heavy-flavor contributions due to charm quarks to the structure function $g_1(x,Q^2)$ due to the Wilson coefficients $\Delta H_g^{\rm S}, \Delta H_q^{\rm PS}, \Delta L_q^{\rm NS}, \Delta L_g^{\rm S}$ and $\Delta L_g^{\rm PS}$ at $Q^2 = 100\ {\rm GeV}^2$ at different cumulative orders in a_s.

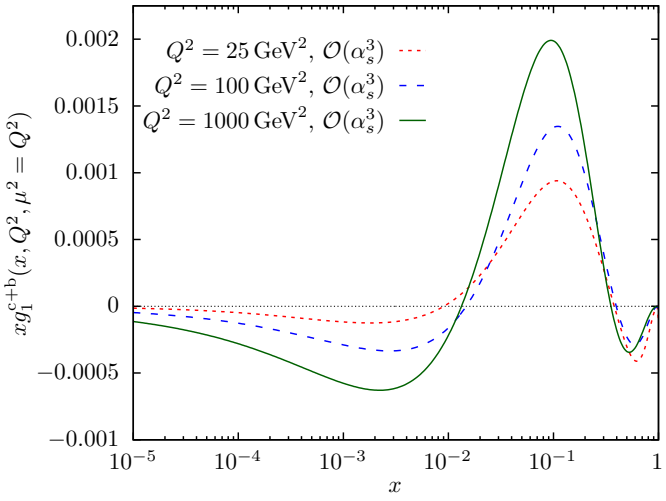

FIG. 7. The heavy-flavor contributions due to charm and bottom quarks to the structure function $g_1(x,Q^2)$ at NNLO.

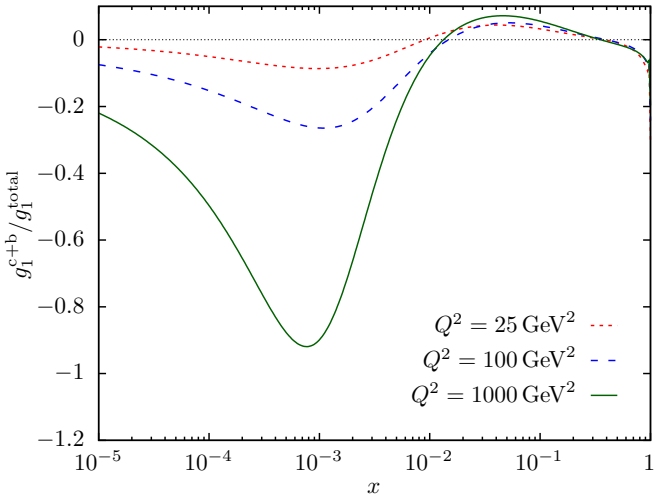

FIG. 8. The ratio of the heavy-flavor contributions due to charm and bottom quarks to the structure function $g_1(x,Q^2)$ at NNLO.

OMEs and the massless three-loop Wilson coefficients, the scheme transformations to the $\overline{\rm MS}$ scheme are not yet known. However, if all contributing quantities, including also the parton distribution functions, are used in this scheme, $g_1(x,Q^2)$, as a scheme independent quantity, can still be assembled. For the process of deep-inelastic scattering, the Larin scheme is a consistent scheme, given the number of contributing γ_5 Dirac matrices. A set of Larin-scheme parton distribution functions has been generated in Ref. [55] and is used in the following illustrations. The massless and massive two-loop corrections for the structure function $g_1(x,Q^2)$ were calculated in Ref. [31].

In Figure 5, we illustrate the scale evolution of the complete structure function $g_1^{\rm total}(x,Q^2)$ from $Q^2 = 25\ {\rm GeV}^2$ to $Q^2 = 1000\ {\rm GeV}^2$ at three-loop order. With growing values of Q^2, $xg_1^{\rm total}(x,Q^2)$ grows below $x \sim 0.2$ and depletes at larger values of x. Also below $x \sim 10^{-2}$ the order in the scales reverts. The structure functions $g_1^{p,d}(x,Q^2)$ are positive within errors, cf. Ref. [56].

Figure 6 illustrates the contributions of the different heavy-flavor Wilson coefficients to g_1^c for $Q^2 = 100\ {\rm GeV}^2$, also with their contributions at different cumulative order in a_s. One clearly sees the importance of the higher order corrections. The largest contribution is due to the gluonic Wilson coefficient $\Delta H_g^{\rm S}$. As has been discussed in Refs. [29, 31], the first moment of $\Delta H_g^{\rm S}(x,Q^2)$ vanishes,

$$\int_0^1 dx \Delta H_g^{\rm S}(x,Q^2) = 0. \tag{10}$$

This is now also found at three-loop order. Mainly due to this, the oscillating structure in Figure 6 is implied. Next in size are the flavor non-singlet and pure-singlet Wilson coefficients, $\Delta L_q^{\rm NS}$ and $\Delta H_q^{\rm PS}$. In the small-x region, the former is positive and the latter negative. $\Delta L_q^{\rm NS}$ turns negative above $x \sim 0.2$ and dominates the large-x region. The contributions due to $\Delta L_g^{\rm S}$ and $\Delta L_g^{\rm PS}$ are smaller but not negligible.

Figure 7 shows the NNLO heavy-flavor contributions to $xg_1(x,Q^2)$. They grow in size with Q^2. Below $x \sim 0.01$ they are negative and turn positive until at $x \sim 0.3$ they turn negative again.

In Figure 8, we show the ratio Eq. (9) of the charm and bottom contributions to the whole structure function $g_1(x,Q^2)$ at NNLO for $Q^2 = 25, 100$ and $1000\ {\rm GeV}^2$. In the small-x region, the corrections are negative. The largest negative values are about -10 %, -25 % and -95 % from $Q^2 = 25, 100$ to $1000\ {\rm GeV}^2$. These large corrections occur in a region in which $xg_1(x,Q^2)$ itself is rather small, see Figure 5. Around $x = 10^{-2}$, the ratio turns positive. At $x = 0.3$ it turns negative again, as in

the unpolarized case. The complete structure function $g_1(x,Q^2)$ remains positive. The strong negative correction in the small-x region is mainly induced by the sum rule of the vanishing first moment of $\Delta H_g^{\rm S}$.

CONCLUSIONS

In this Letter, we present for the first time numerical results for the single-mass three-loop corrections to the unpolarized structure function $F_2(x,Q^2)$ and the polarized structure function $g_1(x,Q^2)$ at twist-2. The asymptotic analytic results on the heavy-flavor Wilson coefficients are correlated to the kinematic region in which the higher-twist contributions can be neglected. Our numerical results illustrate the impact of the different Wilson coefficients and show the changes in the structure functions going from the $O(a_s)$ to the $O(a_s^3)$ corrections. In the unpolarized case, the corrections are large in the small-x region, which is also observed in the polarized case. Here, however, the large corrections emerge in a region where the structure function is small, unlike in the former case. The present results are an important step to allow for consistent QCD analyses of the deep-inelastic World data at the level of NNLO, given the partial results used before for combined singlet/non-singlet data analyses. Our new results will allow to improve the knowledge on the strong coupling constant $a_s(M_Z^2)$, the PDFs and the charm mass, extracted from the deep-inelastic World data.

Acknowledgements. We would like to thank I. Bierenbaum, A. Goedicke (neé Hasselhuhn), S. Klein, C. Raab, M. Round, M. Saragnese and F. Wißbrock for collaboration in earlier projects and thank P. Marquard for discussions. This work was supported by the European Research Council (ERC) under the European Union's Horizon 2020 research and innovation programme grant agreement 101019620 (ERC Advanced Grant TOPUP), the UZH Postdoc Grant, grant no. [FK-24-115] and by the Austrian Science Fund (FWF) Grant-DOI 10.55776/P20347.

[1] S. Bethke *et al.*, *Workshop on Precision Measurements of α_s*, arXiv:1110.0016 [hep-ph].
[2] S. Moch *et al.*, *High precision fundamental constants at the TeV scale*, arXiv:1405.4781 [hep-ph].
[3] S. Alekhin, J. Blümlein and S.O. Moch, Mod. Phys. Lett. A **31** (2016) no.25, 1630023.
[4] D. d'Enterria et al., *The strong coupling constant: State of the art and the decade ahead*, [arXiv:2203.08271 [hep-ph]].
[5] S. Alekhin, J. Blümlein, K. Daum, K. Lipka and S. Moch, Phys. Lett. B **720** (2013) 172–176 [arXiv:1212.2355 [hep-ph]].
[6] A. Accardi *et al.*, Eur. Phys. J. C **76** (2016) no.8, 471 [arXiv:1603.08906 [hep-ph]].
[7] S. Alekhin, J. Blümlein, S. Moch and R. Placakyte, Phys. Rev. D **96** (2017) no.1, 014011 [arXiv:1701.05838 [hep-ph]].
[8] R.D. Ball *et al.* [PDF4LHC Working Group], J. Phys. G **49** (2022) no.8, 080501 [arXiv:2203.05506 [hep-ph]].
[9] M. Buza, Y. Matiounine, J. Smith, R. Migneron and W.L. van Neerven, Nucl. Phys. B **472** (1996) 611–658 [hep-ph/9601302].
[10] I. Bierenbaum, J. Blümlein and S. Klein, Nucl. Phys. B **820** (2009) 417–482 [arXiv:0904.3563 [hep-ph]].
[11] J. Ablinger, J. Blümlein, S. Klein, C. Schneider and F. Wißbrock, Nucl. Phys. B **844** (2011) 26–54 [arXiv:1008.3347 [hep-ph]].
[12] J. Ablinger, A. Behring, J. Blümlein, A. De Freitas, A. Hasselhuhn, A. von Manteuffel, M. Round, C. Schneider and F. Wißbrock, Nucl. Phys. B **886** (2014) 733–823 [arXiv:1406.4654 [hep-ph]].
[13] J. Ablinger, A. Behring, J. Blümlein, A. De Freitas, A. von Manteuffel and C. Schneider, Nucl. Phys. B **890** (2014) 48–151 [arXiv: 1409.1135 [hep-ph]].
[14] A. Behring, I. Bierenbaum, J. Blümlein, A. De Freitas, S. Klein and F. Wißbrock, Eur. Phys. J. C **74** (2014) no.9, 3033 [arXiv:1403.6356 [hep-ph]].
[15] J. Ablinger, A. Behring, J. Blümlein, A. De Freitas, A. von Manteuffel, C. Schneider and K. Schönwald, Nucl. Phys. B **999** (2024) 116427 [arXiv:2311.00644 [hep-ph]].
[16] J. Ablinger, A. Behring, J. Blümlein, A. De Freitas, A. von Manteuffel, C. Schneider and K. Schönwald, Phys. Lett. B **854** (2024) 138713 [arXiv:2403.00513 [hep-ph]].
[17] J. Ablinger, A. Behring, J. Blümlein, A. De Freitas, A. von Manteuffel, C. Schneider and K. Schönwald, Nucl. Phys. B **953** (2020) 114945 [arXiv:1912.02536 [hep-ph]].
[18] J. Blümlein, A. De Freitas, M. Saragnese, C. Schneider and K. Schönwald, Phys. Rev. D **104** (2021) no.3, 034030 [arXiv:2105.09572 [hep-ph]].
[19] E. Witten, Nucl. Phys. B **104** (1976) 445–476.
[20] J. Babcock, D.W. Sivers and S. Wolfram, Phys. Rev. D **18** (1978) 162–181.
[21] M.A. Shifman, A.I. Vainshtein and V.I. Zakharov, Nucl. Phys. B **136** (1978) 157–176, [Yad. Fiz. **27** (1978) 455–469].
[22] J.P. Leveille and T.J. Weiler, Nucl. Phys. B **147** (1979) 147–173.
[23] M. Glück, E. Hoffmann and E. Reya, Z. Phys. C **13** (1982) 119–130.
[24] A.D. Watson, Z. Phys. C **12** (1982) 123–125.
[25] E. Laenen, S. Riemersma, J. Smith and W.L. van Neerven, Nucl. Phys. B **392** (1993) 162–228.
[26] E. Laenen, S. Riemersma, J. Smith and W.L. van Neerven, Nucl. Phys. B **392** (1993) 229–250.
[27] I. Bierenbaum, J. Blümlein and S. Klein, Nucl. Phys. B **780** (2007) 40–75 [arXiv:hep-ph/0703285 [hep-ph]].
[28] I. Bierenbaum, J. Blümlein, S. Klein and C. Schneider, Nucl. Phys. B **803** (2008) 1–41 [arXiv:0803.0273 [hep-ph]].
[29] M. Buza, Y. Matiounine, J. Smith and W.L. van Neerven, Nucl. Phys. B **485** (1997) 420–456 [hep-ph/9608342].
[30] F. Hekhorn and M. Stratmann, Phys. Rev. D **98** (2018) no.1, 014018 [arXiv:1805.09026 [hep-ph]].
[31] I. Bierenbaum, J. Blümlein, A. De Freitas, A. Goedicke, S. Klein and K. Schönwald, Nucl. Phys. B **988** (2023) 116114 [arXiv:2211.15337 [hep-ph]].
[32] M. Buza, Y. Matiounine, J. Smith and W.L. van Neerven, Eur. Phys. J. C **1** (1998) 301–320 [hep-ph/9612398].
[33] J. Ablinger, A. Behring, J. Blümlein, A. De Freitas, A. von Manteuffel, C. Schneider and K. Schönwald, DESY 24–037.
[34] A. Behring, J. Blümlein, A. De Freitas, A. von Manteuffel, K. Schönwald and C. Schneider, Nucl. Phys. B **964** (2021) 115331 [arXiv:2101.05733 [hep-ph]].
[35] J. Ablinger, J. Blümlein, A. De Freitas, A. Hasselhuhn, A. von Manteuffel, M. Round, C. Schneider and F. Wißbrock, Nucl. Phys. B **882** (2014) 263–288 [arXiv:1402.0359 [hep-ph]].
[36] J. Ablinger, A. Behring, J. Blümlein, A. De Freitas, A. Goedicke, A. von Manteuffel, C. Schneider and K. Schönwald, JHEP **12** (2022) 134 [arXiv:2211.05462 [hep-ph]].

[37] J. Blümlein and H. Böttcher, Phys. Lett. B **662** (2008) 336–340 [arXiv:0802.0408 [hep-ph]].

[38] J. Blümlein and H. Böttcher, Proc. of DIS 2012, Bonn, 2012, 237–241, DESY-PROC-2012-02, [arXiv:1207.3170 [hep-ph]].

[39] S. Alekhin, J. Blümlein and S. Moch, Phys. Rev. D **86** (2012) 054009 [arXiv: 1202.2281 [hep-ph]].

[40] J.A.M. Vermaseren, A. Vogt and S. Moch, Nucl. Phys. B **724** (2005) 3–182 [hep-ph/0504242].

[41] J. Blümlein, P. Marquard, C. Schneider and K. Schönwald, JHEP **11** (2022) 156 [arXiv:2208.14325 [hep-ph]].

[42] J. Blümlein and M. Saragnese, Phys. Lett. B **820** (2021) 136589 [arXiv:2107.01293 [hep-ph]].

[43] M. Galassi et al., GNU Scientific Library Reference Manual (3rd Ed.), ISBN 0954612078.
`http://www.gnu.org/software/gsl/`, routine `CQUAD`.

[44] J.A.M. Vermaseren, Int. J. Mod. Phys. A **14** (1999) 2037–2076 [hep-ph/9806280].

[45] J. Blümlein and S. Kurth, Phys. Rev. D **60** (1999) 014018 [hep-ph/9810241].

[46] E. Remiddi and J.A.M. Vermaseren, Int. J. Mod. Phys. A **15** (2000) 725–754 [hep-ph/9905237].

[47] S. Moch, P. Uwer and S. Weinzierl, J. Math. Phys. **43** (2002) 3363–3386 [hep-ph/0110083].

[48] J. Ablinger, J. Blümlein and C. Schneider, J. Math. Phys. **54** (2013) 082301 [arXiv:1302.0378 [math-ph]].

[49] J. Ablinger, J. Blümlein, C.G. Raab and C. Schneider, J. Math. Phys. **55** (2014) 112301 [arXiv:1407.1822 [hep-th]].

[50] J. Ablinger, J. Blümlein, A. De Freitas, M. van Hoeij, E. Imamoglu, C.G. Raab, C.S. Radu and C. Schneider, J. Math. Phys. **59** (2018) 062305 [arXiv:1706.01299 [hep-th]].

[51] J. Blümlein and C. Schneider, Int. J. Mod. Phys. A **33** (2018) 1830015 [arXiv:1809.02889 [hep-ph]].

[52] A. Behring, J. Blümlein and K. Schönwald, JHEP **06** (2023) 062 [arXiv:2303.05943 [hep-ph]].

[53] K.A. Olive *et al.* [Particle Data Group], *Review of Particle Physics*, Chin. Phys. C **38** (2014) 090001.

[54] S.A. Larin, Phys. Lett. B **303** (1993) 113–118 [hep-ph/9302240].

[55] J. Blümlein and M. Saragnese, Phys. Rev. D **110** (2024) no.3, 034006 [arXiv:2405.17252 [hep-ph]].

[56] S. Navas *et al.* [Particle Data Group], Phys. Rev. D **110** (2024) no.3, 030001.